

Resonant growth of stellar oscillations by incident gravitational waves

Yasufumi Kojima[†] and Hajime Tanimoto

Department of Physics, Hiroshima University, Higashi-Hiroshima 739-8526, Japan

Abstract. Stellar oscillation under the combined influences of incident gravitational wave and radiation loss is studied in a simple toy model. The star is approximated as a uniform density ellipsoid in the Newtonian gravity including radiation damping through quadrupole formula. The time evolution of the oscillation is significantly controlled by the incident wave amplitude h , frequency ν and damping time τ . If a combination $h\nu\tau$ exceeds a threshold value, which depends on the resonance mode, the resonant growth is realized.

PACS numbers: 04.30.-w, 04.40.Dg

[†] Email: kojima@theo.phys.sci.hiroshima-u.ac.jp

1. Introduction

Stellar oscillation coupled to gravitational waves is one of important issues for the gravitational wave observatories such as LIGO, VERGO, GEO600 and TAMA. The current status of these detectors is given elsewhere(e.g, [1]). Detection of gravitational radiation from compact stars would provide valuable information about their interior. The frequency and damping time are uniquely affected by the stellar structure. Gravitational wave asteroseismology in the future is also discussed(e.g, [2, 3]). Various oscillation modes in neutron stars have been studied theoretically so far, but little is known of the excitation and damping processes. Most likely event that may excite the oscillations is the birth of the neutron stars after supernova. Some oscillation modes may also be induced by instabilities. An accurate description of these processes requires numerical solution of coupled system of hydrodynamics and the Einstein equations. Recently, the numerical simulations have been developing in the several approaches, e.g, 2D Newtonian simulation[4], 3D smooth particle code simulation[5], Newtonian MHD simulation[6], GR simulation[7] and the referees therein.

Approximate approach is also helpful to get some insight into the physical processes. For example, excitation of neutron star oscillations in a close binary is studied by using following approximation[8, 9, 10, 11]. One of the two stars is an extended body, and the other is approximated by a pointlike particle. The stellar perturbations in general relativity are solved for the extended body, while the pointlike mass moves on geodesic of the spacetime around the star. The oscillation mode can be excited by the particle, whose orbit is close enough to satisfy the resonance condition between normal mode frequency of the star and orbital Kepler frequency. Detailed discussion concerning excitation of neutron star oscillation in this approach may be found in Ref.[11] and references therein. This is one of examples showing that oscillations are excited by the external almost periodic disturbance. The resonant growing mode is in general significantly affected by viscous damping, which may come from physical origins or numerical truncation errors. It is therefore better to examine resonant property in a simplified model. In this paper, we consider an idealized situation to study the resonant behavior. Incident gravitational waves are regarded as external periodic disturbance. The purpose of our study is the following. What is the resonance condition? How does the amplitude grow? The external disturbance is characterized by the frequency, duration and amplitude of the waves. These quantities are closely related with the resonance condition and the amplification of growing mode. The resonance condition is a relation between intrinsic and external frequencies. The amplification factor depends on growth rate of the mode and duration of the disturbances.

This paper is organized as follows. In section 2, we briefly summarize the resonance appeared in a harmonics oscillator, which is helpful to examine the stellar model. In section 3, we consider the stellar oscillation with ellipsoidal model under Newtonian gravity. The gravitational radiation loss is included by the quadrupole formula. We show the numerical results in section 4. Section 5 is devoted to discussion.

2. Resonance in a harmonic oscillator

We here briefly consider the resonance in a harmonic oscillator, which is a useful model to understand the more realistic case below. There are two kinds of resonance (e.g, [12]). One type occurs when the frequency ($= \Omega/2\pi$) of external perturbation matches with the intrinsic frequency ($= \omega/2\pi$), i.e, $\Omega = \omega$. The relevant equation is given by

$$\ddot{X} + \omega^2 X = f \cos(\Omega t). \quad (1)$$

In this case, the amplitude X increases linearly with the time, $X \propto (f/2\Omega)t \sin(\Omega t)$.

Another type of resonance is parametric resonance, which occurs for time-dependent frequency. One example known as the Mathieu's equation is

$$\ddot{X} + \omega^2(1 + b \cos(\Omega t))X = 0. \quad (2)$$

The exponential growth for instability appears when $\omega/\Omega = n/2$, ($n = 1, 2, 3, \dots$). There is allowed range of frequency for each resonance condition, but the width of resonance range decreases rapidly with increasing n . The matching for large n is hardly satisfied. The strongest instability occurs for the fundamental one $n = 1$. Therefore the parametric resonance with $n = 1$ is very important. The growth rate s in $X \propto \exp(st)$ for the fundamental mode can be calculated for small b as

$$s = -\frac{1}{2} \left[-(\Omega - 2\omega)^2 + \frac{1}{4}b^2\omega^2 \right]^{1/2} \sim \frac{1}{4}b\omega \quad (3)$$

for the unstable region

$$-\frac{1}{2}b\omega < \Omega - 2\omega < \frac{1}{2}b\omega. \quad (4)$$

In the presence of frictional damping, the amplitude decreases with time as $\exp(-\gamma t)$. The damping counteracts the parametric resonance, so that the condition is more constrained. The growing solution of the resonance is possible only when b exceeds a threshold $4\gamma/\omega$.

3. Stellar pulsation

Now we consider the pulsation of the star based on Newtonian gravity. The equation of motion for the pulsation driven by external acceleration \vec{g} is

$$\frac{d\vec{v}}{dt} = -\frac{1}{\rho} \vec{\nabla} p - \vec{\nabla} \phi + \vec{g}. \quad (5)$$

As an external perturbation, we consider plane parallel wave with amplitude h and angular frequency Ω , propagating along z -axis. The tidal acceleration by the incident gravitational wave is expressed as[13]

$$\vec{g} = \left[-\frac{1}{2}h\Omega^2 x \cos \Omega(t - z), \frac{1}{2}h\Omega^2 y \cos \Omega(t - z), 0 \right]. \quad (6)$$

We here consider $+$ mode only. Another polarization mode \times is given simply by $\pi/4$ rotation about z -axis, and may be ignored without loss of generality. Deceleration due to quadrupole radiation loss is given by[13]

$$\vec{g} = -\vec{\nabla} \frac{G}{5c^5} \mathcal{I}_{ij}^{(5)} x^i x^j, \quad (7)$$

where $\mathcal{I}_{ij}^{(5)}$ is five time derivatives of reduced quadrupole moment. We incorporate both effects by eqs.(6) and (7).

We are interested in global motion of a star, and therefore approximate it by the ellipsoidal model. In the approximation, the dynamical motion is limited to uniform expansion and compression along three axes. Thus, the fluid motion is described by three functions of time $a_i(t)$ ($i = 1, 2, 3$). The ellipsoidal approximation is often used as a simplified model to extract dynamical features in more realistic cases. (See e.g, [14, 15, 16, 17, 18].) Assuming incompressible fluid with uniform density ρ , the dynamics can be determined by

$$\ddot{a}_1 = -2\pi G \rho a_1 A_1 + \frac{K}{a_1} - \frac{1}{2} h \Omega^2 a_1 \cos \Omega t - \frac{2G}{5c^5} \mathcal{I}_{xx}^{(5)} a_1, \quad (8)$$

$$\ddot{a}_2 = -2\pi G \rho a_2 A_2 + \frac{K}{a_2} + \frac{1}{2} h \Omega^2 a_2 \cos \Omega t - \frac{2G}{5c^5} \mathcal{I}_{yy}^{(5)} a_2, \quad (9)$$

$$\ddot{a}_3 = -2\pi G \rho a_3 A_3 + \frac{K}{a_3} - \frac{2G}{5c^5} \mathcal{I}_{zz}^{(5)} a_3, \quad (10)$$

where the function A_i depends on the shape of the ellipsoid, and is described in [19]. The term K associated with pressure is algebraically determined from the condition $d(\ln(a_1 a_2 a_3))/dt = 0$. The system of eqs.(8)-(10) depends on three dimensionless parameters, $Q = \omega \tau / 2\pi = \nu \tau$, ω / Ω and h , where ν ($= \omega / 2\pi$) is intrinsic frequency of the stellar oscillation, and τ is damping time due to gravitational radiation. The amplitude becomes e^{-1} after Q times oscillations. These values are physically related with mass M and radius R of the star as

$$\omega = \left(\frac{4GM}{5R^3} \right)^{1/2}, \quad \tau^{-1} = \frac{2GMR^2\omega^4}{25c^5}. \quad (11)$$

In order to clarify the dynamics of this system, we assume small deviation from spherically symmetric equilibrium ($a_i = 1$), and linearize eqs.(8)-(10). We neglect the radiation loss for simplicity and limit the oscillation to the toroidal motion in x - y plane. The dynamics can be expressed by a single function X as

$$\ddot{X} + \omega^2 \left(1 + \frac{h}{2} \left(\frac{\Omega}{\omega} \right)^2 \cos \Omega t \right) X = -\frac{1}{2} h \Omega^2 \cos \Omega t, \quad (12)$$

where X represents the deviations δa_i ($= a_i - 1$) from the equilibrium state:

$$\delta a_1 = -\delta a_2 = X, \quad \delta a_3 = 0. \quad (13)$$

Equation (12) is the Mathieu's one with periodic source term. As considered in section 2, it is clear that two kinds of resonance are possible in eq.(12), and hence in the system of eqs. (8)-(10). In the astrophysical situation, periodic external perturbation may be

expected, e.g, in close binary system, where the standard resonance due to the periodic driving force is relevant. On the other hand, we do not definitely know the situation in which the parametric resonance occurs, but the relevant elements may be involved in the complicated system like the hydrodynamical core collapse.

4. Numerical calculation

4.1. Off-resonant case

Before examining the resonant properties of the system (8)-(10), we first of all show the behavior of non-resonant case. This is necessary for checking and comparing models. As for initial conditions of numerical calculations, we adopt static state, i.e, ($a_1 = a_2 = a_3 = 1, \dot{a}_1 = \dot{a}_2 = \dot{a}_3 = 0$). The oscillation amplitudes $\delta a_1, \delta a_3$ as a function of time are shown in Fig.1. The amplitude δa_2 is always well approximated as $\delta a_2 \approx -\delta a_1$, and is omitted in the figure. The parameters adopted for the calculation are $Q = 90$, $\omega/\Omega = 0.6$ and $h = 0.1$. The damping time τ of the model corresponds to $\tau = 2\pi Q/\omega = 150 \times (2\pi/\Omega)$. In the early stage of the oscillation, the temporal profiles are a mixture of two modes with frequencies $\omega (= 0.6\Omega)$ and Ω . There is a modulation of two modes, which causes larger amplitudes of the oscillations due to interference of two waves. As the time goes on, the amplitudes of both modes are damped by the radiation loss. Since the external perturbation with Ω is always supplied, the mode becomes dominant around $\tau (= 150 \times (2\pi/\Omega))$, and the oscillation is eventually enforced to match it at the late phase, typically at several times τ , as shown in right panel of Fig.1. From the numerical results, we found that the motion along a_3 is also induced by the incompressible condition $a_3 = 1/(a_1 a_2)$. This differs from linear analysis, in which a_3 is always constant. The oscillation of δa_3 is of order h^2 in the amplitude, and is induced by a mixture of stellar intrinsic oscillation, ω and external perturbation, Ω . The frequencies of δa_3 are therefore described by $2\Omega, 2\omega$ and $\Omega \pm \omega$.

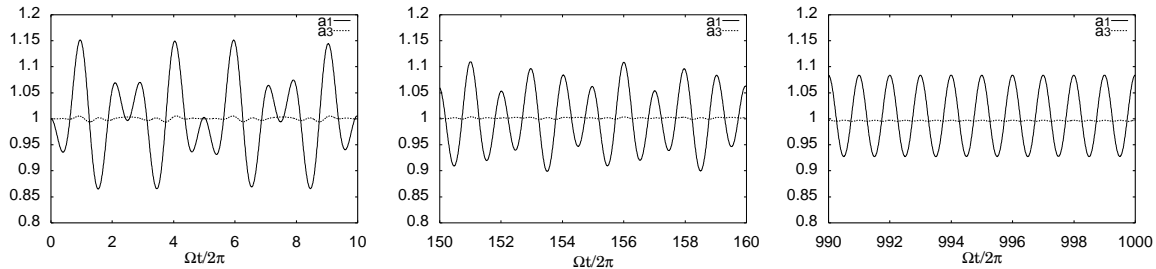


Figure 1. Oscillation amplitudes δa_1 and δa_3 as a function of time $\Omega t/(2\pi)$. Parameters of the model are $Q = 90$, $\omega/\Omega = 0.6$ and $h = 0.1$. From the left to right panels, the amplitudes of the oscillations are shown for the early, middle and late stages.

We have also calculated the oscillations for different parameters, and found that the general behavior is almost the same unless the resonance condition is satisfied.

The temporal behavior may be easily understood by analyzing the numerical data with Fourier transformation. It is found that the oscillation is approximated by the following curve consisted of two frequencies ω and Ω :

$$\delta a_1 \approx -\delta a_2 \approx \frac{\Omega^2 h}{2|\Omega^2 - \omega^2|} (\cos \Omega t - \exp(-t/\tau) \cos \omega t), \quad \delta a_3 \propto h^2. \quad (14)$$

This formula can be derived from the linearized system eq.(12) and the accuracy is checked by fitting the numerical results for a wide range of parameters.

In the limit of $t \rightarrow \infty$, the oscillation with ω in a_1 or a_2 is completely damped, and the mode matched with the incident wave survives with the amplitude $\Omega^2 h / (2|\Omega^2 - \omega^2|)$. The amplitude of the steady state realized at $t \rightarrow \infty$ becomes larger when $\Omega \rightarrow \omega$. The amplitude apparently diverges at the resonance, but does not actually, because even small dissipation is important and suppresses the divergence in that case. See section 4.3.

4.2. Parametric resonance of fundamental mode

In this section, we consider the parametric resonance of the fundamental mode by setting $\omega/\Omega = 1/2$. In Fig.2, we show time evolution of the model with $h = 0.1$, $Q = 45$. The damping time τ corresponds to $\tau = 90 \times (2\pi/\Omega)$. In the early phase of the time evolution, the amplitude of intrinsic stellar oscillation mode $\omega (= \Omega/2)$ exponentially grows up. After a hundreds of the oscillations, damping effect becomes important around $t \sim \tau$. Eventually the mode ω is damped, and oscillation is enforced to external mode with Ω at the late phase $t \gg \tau$, in which the amplitude of δa_1 becomes $\delta a_1 \approx 2h/3$. This behavior in the final steady state is the same as that in off-resonant case. Compare the right panel in Fig.1 ($t \approx 1000 \times (2\pi/\Omega)$) with that in Fig.2 ($t \approx 700 \times (2\pi/\Omega)$). Both figures show the behavior corresponding to several times τ . Thus, the parametric excitation decays away in this case.

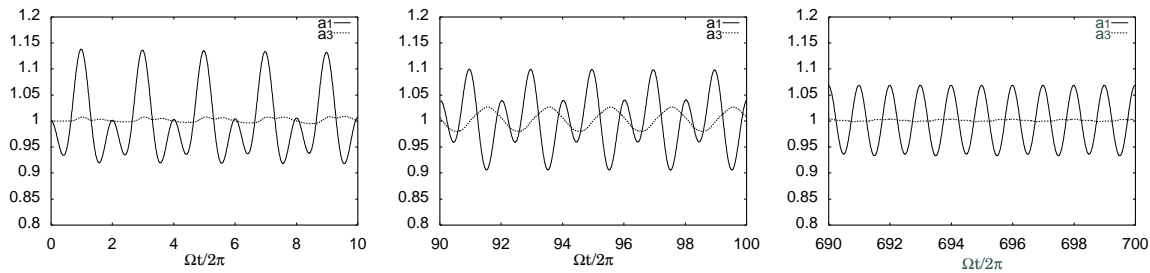


Figure 2. Oscillation amplitudes δa_1 and δa_3 as a function of time $\Omega t / (2\pi)$. Parameters of the model are $Q = 45$, $\omega/\Omega = 0.5$ and $h = 0.1$.

We consider a case in which the radiation loss is less effective. The results for the parameters $h = 0.1$, $Q = 75$ are shown in Fig.3. The damping time τ corresponds to $\tau = 150 \times (2\pi/\Omega)$. In the early stage, a mixture of two frequencies $\omega (= \Omega/2)$ and Ω can be seen. There are no drastic differences between the left panels in Fig.2 and Fig.3 as

for the early stages $t < \tau$. By comparing the right panels in Fig.2 and Fig.3, it is found that the parametric excitation occurs in Fig.3, since the oscillation amplitudes of both δa_1 and δa_3 are indeed enhanced. The dominant oscillation frequency at the later stage is determined by not external one Ω , but intrinsic one ω . The frequency of δa_3 is also ω , which comes from quadratic coupling between Ω and ω , as $\Omega - \omega (= \omega)$. The other higher frequencies such as 2ω , $\Omega + \omega (= 3\omega)$ and $2\Omega (= 4\omega)$ are less excited. The amplitude at the later stage is saturated around the value $\delta a_1 \approx \delta a_3 \approx 4h$, which is several times larger than that of off-resonant oscillation. This saturation property is quite different from the linear theory, in which the amplitude of the unstable mode exponentially increases so far as resonant condition is satisfied. In the nonlinear ellipsoidal model, the motion along the longitudinal direction a_3 plays a key role on the saturation as explained below. The amplitudes of δa_1 and δa_2 grow in proportion to h , while that of δa_3 , which is formally $\sim h^2$, also grows due to nonlinear coupling. The amplitude of δa_3 is given by $\delta a_3 \sim (\delta a_1)^2$. When the oscillation amplitude becomes large enough, say $\delta a_1 \sim 0.5$, δa_3 is also large enough. The motion of δa_3 is no longer neglected and significantly affects the dynamics of δa_1 and δa_2 . In presence of the dynamics of δa_3 the growing amplitudes are saturated around the same order $\delta a_1 \sim \delta a_2 \sim \delta a_3 \sim 0.5$.

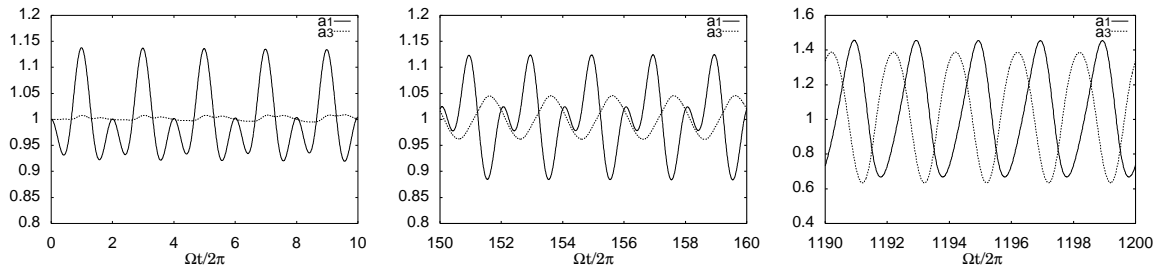


Figure 3. Oscillation amplitudes δa_1 and δa_3 as a function of time $\Omega t/(2\pi)$. Parameters of the model are $Q = 75$, $\omega/\Omega = 0.5$ and $h = 0.1$.

So far we have shown two different results of the resonance in Fig.2 and Fig.3. The parametric oscillation is excited for weak damping case, i.e, large Q , while it decays out for strong damping case, i.e, small Q . The excitation condition should also depend on the amplitude h of the incident gravitational wave. In order to study the resonance condition for $\omega/\Omega = 1/2$, we have performed the numerical calculations of eqs.(8)-(10) for various parameters (h, Q) , typically in the range $20 < Q < 200$. The results are summarized in Fig.4.

We found that a combination of the parameters, hQ is a very important factor to determine the evolution[‡]. As shown in Fig.4, there is a critical curve discriminating between growth and damped cases. The curve is empirically given by $hQ \approx 7$. Below the critical curve, the damping effect is so strong that the parametric excitation is suppressed like in Fig.2. On the other hand, above the critical curve, the damping

[‡] Note that hQ corresponds to $b\omega/\gamma$ in the harmonics oscillator shown in section 2. The importance of this factor is reasonable.

effect is less effective. In this case, parametric excitation of the intrinsic oscillation with ω occurs and the amplitudes can grow up. Eventually, the nonlinear effect becomes important and the amplitudes of the unstable oscillations are saturated around finite values.

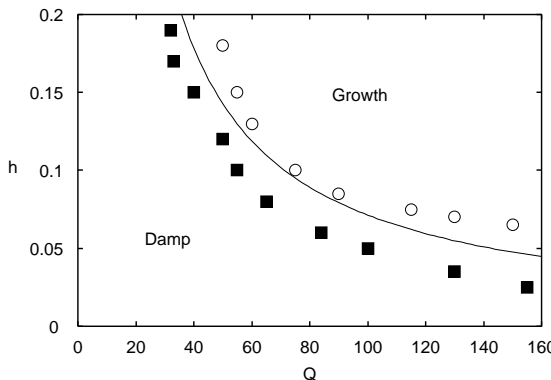


Figure 4. Excitation of the resonant oscillation significantly depends on the parameters, Q and h . Open circles and filled squares respectively denote growth and damped cases in the final steady states. The critical curve discriminating two states is approximately given by $hQ \approx 7$.

4.3. Resonance at $\omega = \Omega$

In this section, we consider the resonant behavior at $\omega = \Omega$. Two typical cases are shown in Fig.5 and Fig.6. These figures show their long term evolutions up to hundreds of cycles of the oscillations, so that each sinusoidal curve is not clear, but the gradual change of the envelope is seen. The model parameters of Fig.5 are $Q = 100$, $h = 5 \times 10^{-3}$, while those of Fig.6 are $Q = 100$, $h = 5 \times 10^{-2}$. The behaviors are the same only for the initial stages, in which the amplitude of δa_1 (or δa_2) increases linearly with time: $\delta a_1 \approx h\Omega t \sin(\Omega t)/4$, so far as $\delta a_1 \ll 1$. The later behaviors significantly depend on the adopted parameters, and are exhibited in quite different way. We have also calculated in a wide range of parameter space (Q, h) and found that the most important factor is hQ like in the previous section. The reason is explained below.

The oscillation of δa_3 is inevitably induced by the nonlinear coupling: $\delta a_3 \propto \delta a_1 \delta a_2 \sim (h\Omega t)^2 \sin^2(\Omega t)/16$. The amplitude of δa_3 grows quadratically with time, and is therefore small only in the initial evolution. There is an epoch in which both amplitudes of δa_1 and δa_3 become the same order. This non-linear timescale t_n is estimated as $t_n = 4/(h\Omega)$ by setting $\delta a_1 = \delta a_3$, if the damping may be neglected. It is important to compare this timescale with that of the radiation loss $\tau = Q \times 2\pi/\Omega$. If $\tau < t_n$, which corresponds to $hQ < 2/\pi \approx 0.6$, the radiation loss controls the evolution. As shown in Fig.5 ($hQ = 0.5$), the grown amplitude of δa_1 is saturated around the value $\delta a_1 \sim h\Omega\tau \sim hQ$. The amplitude of δa_3 grows up in much longer nonlinear timescale, which is not exactly but roughly given by t_n . We have shown in Fig.5 the time evolution

for $t < 250 \times (2\pi/\Omega)$, but confirmed that the subsequent evolution for $t > 250 \times (2\pi/\Omega)$ becomes almost steady state with some small modulation in the amplitudes.

On the other hand, if $\tau > t_n$, i.e., $hQ > 2/\pi$, the nonlinear coupling is important. The behavior in this case is highly unstable as shown in Fig.6 ($hQ = 5$). The amplitudes δa_i ($i = 1, 2, 3$) become $\mathcal{O}(1)$. The nonlinear timescale in this model corresponds to $t_n \sim 13 \times (2\pi/\Omega)$, where the amplitude δa_3 becomes large. The time evolution exhibits *chaotic behavior*§, and therefore the accurate numerical integration is rather difficult for much longer time, say, up to $10^3 \times (2\pi/\Omega)$ in Fig.6.

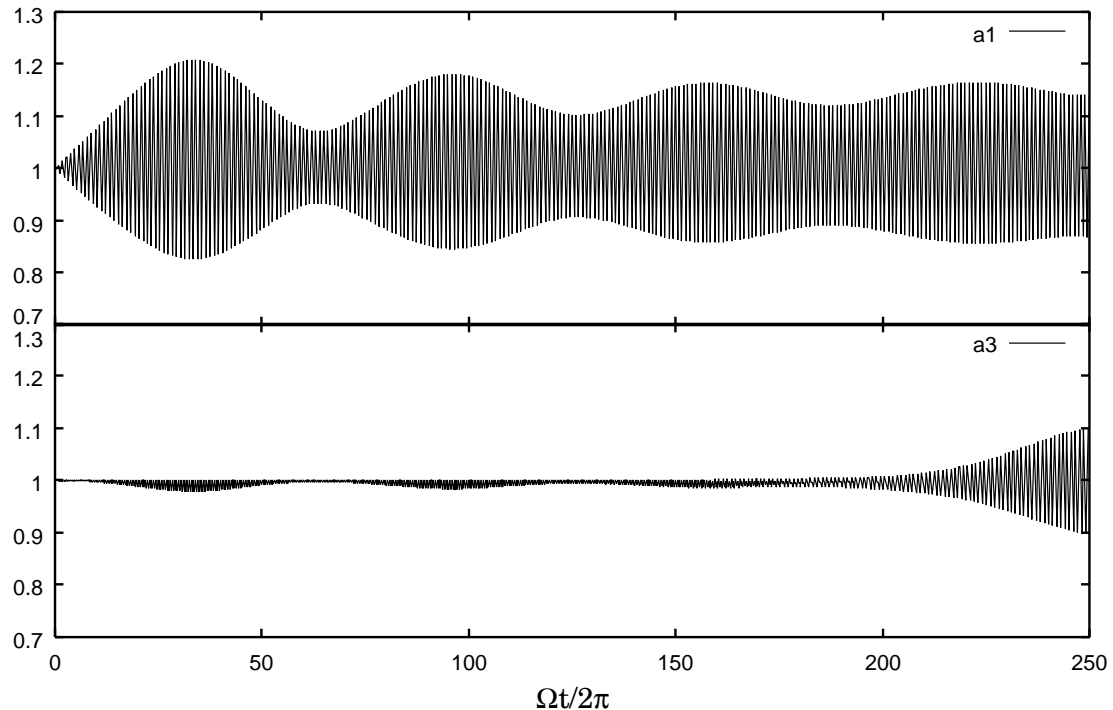


Figure 5. Oscillation amplitudes δa_1 and δa_3 as a function of time $\Omega t/(2\pi)$. Parameters of the model are $Q = 100$, $\omega = \Omega$ and $h = 5 \times 10^{-3}$

5. Summary and discussion

In this paper, we have examined resonant oscillations in ellipsoidal stellar model with incoming gravitational wave. Resonance occurs when a certain matching condition holds between the stellar oscillation and the external periodic disturbance. In the presence of radiation loss, the evolution significantly depends on a combination $hQ = h\nu\tau$ consisted of the wave amplitude h , frequency ν and the damping time τ . The parametric resonance of the fundamental mode can grow up only if the quantity hQ is larger than a critical

§ In general, it may be necessary to measure e.g, Lyapunov exponent in order to judge whether the nonlinear behavior is chaotic or not. We did not calculate the exponent, but found that the numerical behavior is very sensitive like chaotic system.

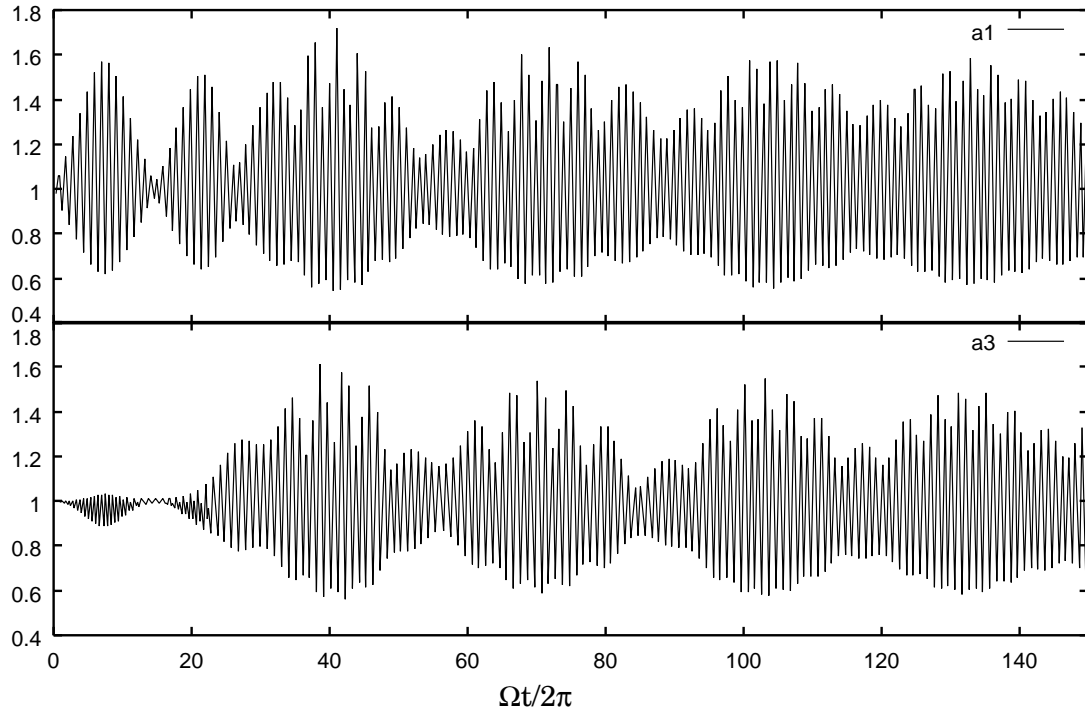


Figure 6. Oscillation amplitudes δa_1 and δa_3 as a function of time $\Omega t/(2\pi)$. Parameters of the model are $Q = 100$, $\omega = \Omega$ and $h = 5 \times 10^{-2}$

value (≈ 7). The amplitude of stellar oscillation increases, but is saturated due to non-linear coupling, by which energy is transferred to the additional oscillatory motion. This point differs from linearized system, in which the amplitude exponentially grows up. If the quantity hQ is smaller than the critical value, the resonant oscillation is damped. The resonant behavior at $\omega = \Omega$ is also determined by the parameter hQ . If hQ is larger than a critical value (≈ 1), then the system exhibits chaotic behavior. We have also performed numerical calculations to explore the possibility of parametric resonance in higher modes $\omega/\Omega = n/2$ ($n = 3, 4, \dots$), and found that the higher modes are much more difficult to be excited.

In our idealized model, the external perturbation is assumed to be constant. This corresponds to the situation that duration t_c of the driving source is much larger than radiation damping time τ , or non-linear time scale t_n . If this condition does not hold, then the environmental effect would appear first in the evolution. For example, when the external perturbation stops at t_c , the enhancement by the resonance also stops there, and the amplitude is subsequently damped around $\tau (> t_c)$.

We now consider the astrophysical relevance of the resonant oscillations. The f-mode oscillation of a neutron star is estimated as the frequency $\nu =$ a few kHz, the damping time $\tau =$ a few $\times 10^{-1}$ s, and therefore $Q \approx 10^2$. In this case, the exotic case needs large amplitude of the gravitational wave $h > Q^{-1} \approx 10^{-2}$. The condition is realized only in hydrodynamical regime, e.g, in core collapse of supernova and in the

final phase of binary coalescence. The duration of periodic disturbance is also important factor. Typically, the timescale is of order 10^{-3} s, and may be too short for the mode to excited. Anyway, more realistic simulation is needed.

Our result may be scaled to the excitation of the f-mode in white dwarfs. In this case, the frequency and damping time are given by $\nu \sim 0.1\text{Hz}$, $\tau \sim 10^{11}\text{s}$, and therefore $Q \sim 10^{10}$. In this case, the condition for the exotic case becomes less severe $h > 10^{-10}$. The region available for this large amplitude may be estimated by the total amount of the radiated energy ΔMc^2 . The distance from the periodic gravitational wave source is still limited to $r \sim G\Delta M/(hc^2) \ll 1\text{pc}$.

Acknowledgments

This work was supported in part by the Grant-in-Aid for Scientific Research (No.14047215, No.16029207 and No.16540256) from the Japanese Ministry of Education, Culture, Sports, Science and Technology.

References

- [1] *Proceedings of the 8th Gravitational Wave Data Analysis Workshop 2004 Class. Quantum Grav.* **21** No 20
- [2] Andersson N and Kokkotas K D 1998 *Mon. Not. R. Astron. Soc.* **299** 1059
- [3] Benhar O, Ferrari V and Gualtieri L 2004 *Phys. Rev. D.* **70** 124015
- [4] Ott C D, Burrows A, Livne E and Walder R 2004 *Astrophys. J.* **600** 834
- [5] Fryer C L, Holz D E, and Hughes S A 2004 *Astrophys. J.* **609** 288
- [6] Kotake K, Yamada S, Sato K, Sumiyoshi K, Ono H and Suzuki H 2004 *Phys. Rev. D.* **69** 124004
- [7] Shibata M and Sekiguchi Y 2004 *Phys. Rev. D.* **69** 084024
- [8] Kojima Y 1987 *Prog. Theor. Phys.* **77** 297
- [9] Ruoff J, Laguna P and Pullin J 2001 *Phys. Rev. D.* **63** 064019
- [10] Tominaga K, Saijo M and Maeda K 2001 *Phys. Rev. D.* **63** 124012
- [11] Pons J A, Berti E, Gualtieri L, Miniutti G and Ferrari V 2002 *Phys. Rev. D.* **65** 104021
- [12] Landau L D and Lifshitz E M 1976 *Mechanics* (Oxford:Pergamon Press)
- [13] Misner C M, Thorne K S and Wheeler J A 1973 *Gravitation* (San Francisco:Freeman)
- [14] Rossner L F 1967 *Astrophys. J.* **149** 145
- [15] Press W H and Teukolsky S A 1972 *Astrophys. J.* **181** 513
- [16] Miller B D 1974 *Astrophys. J.* **187** 609
- [17] Carter B and Luminet J P 1985 *Mon. Not. R. Astro. Soc.* **212** 23
- [18] Lai D, Rasio F A and Shapiro S L 1994 *Astrophys. J.* **437** 742
- [19] Chandrasekhar S 1969 *Ellipsoidal Figures of Equilibrium* (New Haven: Yale Univ. Press)